




## A multi-dimensional validation strategy of pharmacological effects of Radix Isatidis Mixtures against the co-infection of *Mycoplasma gallisepticum* and *Escherichia coli* in poultry

Xiaodi Jin<sup>a,#</sup>, Jinhai Huo<sup>b,#</sup>, Yecheng Yao<sup>a</sup>, Rui Li<sup>a</sup>, Mengqing Sun<sup>a</sup>, Jichang Li<sup>a</sup> , Zhiyong Wu<sup>a,b,\*</sup>

<sup>a</sup> College of Veterinary Medicine, Northeast Agricultural University, 600 Changjiang Road, Xiangfang District, Harbin 150030, PR China

<sup>b</sup> Institute of Chinese Materia Medica, Heilongjiang Academy of Chinese Medicine Sciences, Harbin 150036, PR China

### ARTICLE INFO

#### Keywords:

Radix Isatidis Mixtures  
Omics  
Multi-target  
Co-infection  
Molecular docking

### ABSTRACT

Natural drugs possess exceptional pharmacological properties, yet their development is often hindered by a lack of clarity regarding the mechanisms of their pharmacological actions. Building on our previous research, we employed a co-infection model with *Mycoplasma gallisepticum* (MG) and *Escherichia coli* (*E. coli*) to investigate the pharmacological action of Radix Isatidis Mixtures (RIM). To further demonstrate the various mechanisms underlying the pharmacological effects of RIM, we conducted a validation study focusing on gene expression, protein interactions, metabolic pathways, and molecular docking. Through a multi-omics joint analysis network, we identified key targets and metabolites associated with co-infection and conducted targeted verification experiments with RIM aqueous extracts. The experimental results indicated that, compared to the co-infection group, the RIM treatment group significantly modulated the expression of select genes and proteins, particularly MMP2 and TLR4, with a high level of statistical significance ( $p < 0.01$ ). At the metabolic level, the treatment group exhibited significantly reduced expression levels of Dopamine and  $\gamma$ -Aminobutyric acid. Notably, the molecular docking results highlighted compounds with the most favorable binding affinities: Salvianolic acid A ( $-10.1$  kcal/mol), Licorice ( $-9.3$  kcal/mol), and Isoglycyrrhiza ( $-8.7$  kcal/mol). In conclusion, our multi-level experiments demonstrated that RIM possesses the characteristics of multi-pathway and multi-target treatment for co-infection.

### Introduction

Livestock production, particularly the rearing of domestic chickens, plays a crucial socio-economic role for populations in low-income countries across Africa and Asia (Moazeni, et al., 2016; Mohammadi-far, et al., 2014). They provide high-quality protein and income for impoverished rural households, making them the most commonly kept livestock species worldwide (Mohammadabadi, et al., 2010; Mohammadifard and Mohammadabadi, 2018). Co-infection often occurs due to the problems of environment (Sun, et al., 2023), feeding and pathogens. Respiratory diseases in the poultry industry are among the most intricate challenges (Hu, et al., 2020; Kenton and Production, 2012), characterized by high infection rates, high mortality, and complex etiologies (Wu, et al., 2020; Zhang, et al., 2020). These diseases significantly impact and

constrain the growth of the poultry sector (Rehman, et al., 2022; Umar, et al., 2019). The causative agents include a spectrum of etiologies such as bacteria, mycoplasma, viruses, and immune-suppressing pathogens (Ishfaq, et al., 2020; Mol, et al., 2019; Plichta, et al., 2019; Umar, et al., 2018). Notably, infections with *Mycoplasma gallisepticum* (MG) and *Escherichia coli* (*E. coli*) are prevalent (Awad, et al., 2019), with co-infections being more common than single pathogen infections (Sid, et al., 2015; Telli, et al., 2022). Clinical misdiagnosis and mistreatment are frequent, potentially leading to the overuse of antibiotics and increased health risks (Bai, et al., 2018; Gharibi, et al., 2018; Li, et al., 2023).

To mitigate the risks associated with antibiotic use, recent research efforts are focusing on the development of alternative drugs that can serve as substitutes for antibiotics. For example, the use of probiotics can

\* Corresponding author at: College of Veterinary Medicine, Northeast Agricultural University, 600 Changjiang Road, Xiangfang District, Harbin 150030, PR China.

# Authors equally contributed to this work.

E-mail address: [wuzhiyong@neau.edu.cn](mailto:wuzhiyong@neau.edu.cn) (Z. Wu).

<https://doi.org/10.1016/j.psj.2024.104576>

Received 8 August 2024; Accepted 21 November 2024

Available online 24 November 2024

0032-5791/© 2024 The Authors. Published by Elsevier Inc. on behalf of Poultry Science Association Inc. This is an open access article under the CC BY-NC-ND license (<http://creativecommons.org/licenses/by-nc-nd/4.0/>).

an alternative to antibiotics in livestock and poultry production has produced safer meat products (Gul and Alsayegh, 2022). Furthermore, the utilization of plant extracts has transformed existing breeding concepts. For instance, the use of linseed has been shown to enhance the production performance of lambs (Amirteymoori, et al. 2021). Medicinal plants exhibit significant potential for application within the livestock and poultry industries. Holistic, multi-component, and multi-target research methods offer a more robust theoretical foundation for understanding the pharmacological effects of botanicals. (Wang, et al., 2019). The use of natural products in drug discovery has expanded beyond traditional applications, with advancements in research technology (Ji, et al., 2013; Langeder, et al., 2020; Wang, et al., 2011). For instance, Cao et al. employed metabolomics and transcriptomics to elucidate the hepatoprotective mechanism of Zexie-Baizhu (ZXBZ) decoction through regulation of fatty acid oxidation (FAO) (Cao, et al., 2022). Zheng et al. utilized metabolomics and proteomics to identify disease-related biomarkers (Zheng, et al., 2017). Systems biology and polypharmacology in the context of traditional Chinese medicine (TCM) and complex diseases enable a deeper molecular understanding of cellular and organ behavior, facilitating the identification of active TCM components and the discovery of novel biomarkers (Jin, et al., 2019; Pan, et al., 2020; Sanchez-Vidana, et al., 2017). The integrated "multi-gene-multi-target-complex disease" model offers a more comprehensive reflection of drug action mechanisms and provides innovative validation for TCM development.

In our prior work, we established a co-infection model with MG and *E. coli* and screened six herbal preparations for their therapeutic efficacy against co-infections (Bao, et al., 2022; Wu, et al., 2019). However, the molecular roles of these six herbs in treating co-infections remain to be clarified. This study aims to conduct a targeted verification of the pharmacological action mechanisms of six mixed traditional Chinese medicines, examining them at four levels: genes, proteins, metabolites, and molecular docking, building upon previous research. Our objective is to delineate the molecular pharmacological mechanisms of RIM and to highlight its multi-target and multi-pathway therapeutic characteristics.

## Materials and methods

### Chemicals and reagents

Nutrient Broth was purchased from Beijing Aoboxing BIO-TECH Co. (Beijing, China). Six herbs were purchased from Runhe Chinese medicine processing plant Ltd. Trizol reagent was purchased from Invitrogen Inc., Carlsbad, CA, United States. Reverse transcription kit was purchased from Takara Biotechnology (Beijing, China). BCA protein assay kit was purchased from Wanlei Biotechnology (Liaoning, China). All the primary antibodies were purchased from Bioss Bioscience Inc. (Beijing, China). Enhanced chemiluminescence (ECL) reagent was purchased from Tanon (Shanghai, China). Three metabolite standards is as follows, Dopamine (BD161397, Bide Pharmatech Ltd., Shanghai, China),  $\gamma$ -Aminobutyric (P10002, APEBIO, USA), Leukotriene C4 (GC18663, GLPBIO, USA).

### Bacterial culture and experimental animal source

R<sub>low</sub> strain was obtained from the Harbin Institute of Veterinary Medicine in China, which was grown in a Modified Hayflicks medium. *Escherichia coli* O78 was isolated in our laboratory and cultured in Nutrient Broth (Beijing Aoboxing BIO-TECH Co., Ltd.) (Wu, et al., 2019). The concentration of MG and *E. coli* were  $1 \times 10^9$  CCU/mL and  $10^9$  CFU/mL respectively. The detection of the density was consistent as explained in our previous study (Ishfaq, et al., 2019; Wang, et al. 2021).

120 White Leghorn chickens were purchased from Chia Chau Chicken Farm (Harbin, Heilongjiang, China). The animals were housed in an environment with a temperature of  $25 \pm 2^\circ\text{C}$ , humidity of  $55 \pm 10\%$ , absence of specific pathogens, light/darkness for 12 h each, and

were provided with ad libitum access to food and water.

### Preparation of mixed herbs

Based on previous study, the composition and matching ratio of six herbs were determined, and water extract treatment showed good therapeutic effect (Bao, et al., 2022). Six herbs were purchased from Runhe Chinese medicine processing plant Ltd. Aqueous extract of RIM was prepared as the following procedure. The medicinal materials were mixed in proportion and were macerated for 1 h in ten folds distilled water (v/w), and then decocted for 1 h, after which the filtrate was collected and the residue was decocted again for 1 h up to six folds (v/w) in distilled water. The filtrates were mixed and condensed and then dried by vacuum-drier at  $60^\circ\text{C}$  (Kou, et al., 2005; Yin, et al., 2016). The final concentration of the aqueous extract is 1 mg/mL.

### UHPLC-QTOF-MS analysis for components quantification

LC separation was performed on the Nexera UHPLC LC-30A system (SHIMADZU, Japan) with a Waters BEH C18 column ( $1.7 \mu\text{m} \times 2.1 \times 100$  mm, Waters, USA). Mobile phases, water with 0.1 % formic acid (A) and acetonitrile (B), were applied with gradient elution and the flow rate was kept at 0.4 mL/min. AB 5600 Triple TOF system (SCIEX, USA) was used to collect primary and secondary MS data based on IDA function under the control software (Analyst TF 1.7 (AB Sciex). Instrument dependent parameters: curtain gas = 35 psi, IonSpray voltage = +5500 (POS)/ -4000 (NEG) V, nebulizer gas = 55 psi, heater gas = 55 psi, source temperature =  $550^\circ\text{C}$ . The original mass spectrometry data was imported using Progenesis QI software (Waters Corporation). The corresponding RIM metabolic database in the compound was established, and the peaks containing MS/MS data were identified by the self-built secondary mass spectrometry database (Biotree Biomedical Technology Co., LTD, China).

### RIM treatment and groupings

All the chickens were divided randomly into 4 groups. Each group has 30 as follows. Control group (A): Chickens in the CG were fed only with basal diet and inoculated with the culture medium 0.2 mL on day 7 in air sac; Co-infection group (B): The Co-infection model was constructed as previously (Wu, et al., 2019), 0.2 mL of MG medium ( $1 \times 10^9$  CCU/mL) was injected into the left caudal thoracic air sac on the 7th day, and 0.1 mL of *E. coli* bacteria ( $10^9$  CFU/mL) was injected intraperitoneally on day 10; Co-infection + RIM administration group (C): The same infection model as mentioned above, and treated with the aqueous extract of RIM orally by gavage. The treatment started on day 13 and continued for 5 days, once a day at a dose of 450 mg/kg; RIM control group (D): The same dose of RIM (450 mg/kg) was given orally to chickens by gavage started at day 13 and continued for 5 days. On the 18th day, 20 chickens from each group were euthanized using the method of cardiac blood collection. Lung and serum samples in each group were collected for further analysis. All the samples were placed in sterile DNase- and RNase-free centrifuge tubes (Axygen, USA), directly frozen with liquid nitrogen, and subsequently stored at  $-80^\circ\text{C}$ .

### Joint pathway analysis

16 serum samples of Control and Co-infection groups were examined by the LC-MS system as explained in our previous study (Wu, et al., 2020). Differentially expressed metabolites (DEMs) were screened in combination with univariate analysis of fold change and q-value. Screening conditions: 1)  $\text{VIP} \geq 1$ ; 2) fold change  $\geq 1.2$  or  $\leq 0.8333$ ; 3)  $\text{p-value} < 0.05$ . The DEMs and the previous target gene symbols (Supplementary material 1) were imported into the MetaboAnalyst (MetaboAnalyst v4.0), which could simultaneously analyze genes and metabolites of interest within the context of metabolic pathways

(Chong, et al., 2018; Chong, et al., 2019).

#### Quantitative RT-PCR examination

The 100 mg lung samples were obtained from three different animals in the each group. Total 12 lung tissue samples were homogenized for 2 min at a low frequency of 65 Hz using an automatic tissue homogenizer machine (Shanghai Jingxin Industrial Development Co., Ltd.). Total RNA was extracted using Trizol reagent (Invitrogen Inc., Carlsbad, CA, United States) and the reverse transcription of cDNA was performed according to the manufacturer's instructions (Takara Biomedical Technology (Beijing) Co., Ltd.). The quantity and quality of extracted RNA and synthesized cDNA were determined by ultraviolet spectroscopy using a spectrophotometer (NanoDrop ND-1000; Thermo Fisher Scientific, DE, USA). The RNA had an OD 260/OD 280 ratio >1.9; cDNA 260/230 ratio > 1.9. The primer sequences are shown in Table 1. All primers were designed and synthesized by Sangon Biotech (Shanghai, China). Quantitative RT-PCR was performed to analyze gene expression using a LightCycler96 (Roche, Basel, Switzerland). Each treatment had three biological replicates and three technical replicates. The fold change in gene expression was calculated using the  $\Delta\Delta$  cycle time (Ct) method after the expression level was normalized with the GAPDH gene taken as an internal standard.

#### Western blotting of targets genes

Western blotting was used to measure the related target proteins. Total proteins of lung tissues were extracted by the whole-cell lysis assay and the supernatant protein content was determined using the BCA protein assay kit (Wanlei, Liaoning, China). The membranes were incubated overnight on a shaker at 4°C with primary antibodies against  $\beta$ -actin (1:5000 dilution), MMP2 (1:500 dilution), TLR4, c-FOS, BDKRB1, VEGFA, and EDN-1 (1:1000 dilution). All the primary antibodies purchased from Bioss Bioscience Inc. (Beijing, China), and species homology included *Gallus gallus*. Secondary anti-mouse and anti-rabbit IgG peroxidase were used for 1 h, and then bound immune-complexes were detected using enhanced chemiluminescence (ECL) detection. The protein bands were analyzed by densitometry using Image J (V 1.42, National Institutes of Health, USA).

**Table 1**  
Primers used for QRT-PCR analysis of target genes.

Name	Accession number	Primer	Tm
NOS2	NM_204961.2	F: CAGCTGATGGGTGTGGAT R: TTTCTTTGGCTACGGGTC	55.8°C
MYC	NM_001030952.2	F: CCATCATCATCCAGGACTGC R: TTGGTAGTGGCGAGCTTCT	58°C
TLR4	NM_001030693.2	F: TGCCATCCCAACCCACACAG R: ACACCCACTGAGCAGCACCAA	63.5°C
MMP2	NM_204420.3	F: AAACCTACCAGCCTGGACTAC R: CTCATTCCAAGAATCCGCAATG	59.9°C
VEGFA	NM_205042.3	F: CAATTGAGACCCTGGTGGAC R: TCTCATCAGAGGCACACAGG	57.2°C
EDN1	MK139007.1	F: GCCAGCCAGAGACAAGAA R: TGAGCCCAGAGATCTTTTCC	57.6°C
BDKRB1	NM_001080720.2	F: GTACCCAAGTGTATCGACGCCATC R: GCGACAGCCAGGTTCAACAAGG	64.7°C
HRH3	XM_040687801.2	F: GCTCTGCTGATCGCCGTAC R: GCCAGTTGAGGAGGAAGAAGTTG	63.8°C
CHRM4	NM_001398169.1	F: AGCCAGGAGGACCAAGATG R: TGCCACAATGAAGTCCAGAAC	65°C
VAMP2	XM_040679081.2	F: ATGTCTGCTCCAGCTCCTACCC R: CATCCACTTGGGCTTGGCTCTG	62.2°C
IFNG	NM_205149.2	F: ACAAGTCAAAGCCGCACATCAAAC R: TTTACCTTCTTACGCCATCAGG	65.4°C
FOS	NM_205508.1	F: ACCTACACTCCACCTTCGTCTTC R: GTTGCTGCTGCTGCCCTTCC	62.8°C
GAPDH	NM_204305.1	F: CAGAACATCATCCAGCGTCCAC R: CGGCAGGTCAAGTCAACAACAG	66.2°C

#### Detection of major metabolites by LC-MS

Three key metabolites (Dopamine,  $\gamma$ -Aminobutyric acid, and Leukotriene C4) were obtained from the results of the joint analysis, and the LC-MS method was used for the detection and quantification of targeted metabolites in the anion mode. We first prepared the serum samples and standards for pretreatment by organic precipitation. The information of the three metabolite standards is as follows, Dopamine (BD161397, Bide Pharmatech Ltd., Shanghai, China),  $\gamma$ -Aminobutyric (P10002, APEBIO, USA), Leukotriene C4 (GC18663, GLPBIO, USA). The mobile phases of Dopamine and  $\gamma$ -Aminobutyric acid were A: 20 mM ammonium formate solution (0.1 % formic acid), B: methanol. While, the mobile phases of Leukotriene C4 were: A (0.1 % formic water), B (0.1 % acetonitrile formate). Then, the Agilent 6490 QQQ mass spectrometer (Agilent Technologies, England) was conducted to obtain the primary and secondary mass spectrometer data based on MRM mode and adopted positive mode. The parameters of the ESI ion source were set as follows: GasTemp: 200°C, GasFlow: 12 L/min, SheathGasFlow: 12 L/min, SheathGas Temp: 350°C. Capillary voltage (VCap): 4000 V. Finally, by using the Mass Hunter Workstation Quantitative (Agilent Technologies, England), the sample concentration was calculated by using the standard product response and corresponding concentration as the standard curve by a single point method.

#### Predictive models and molecular docking

A total of 12 target proteins were selected considering their key roles in RIM treatment. According to the results of the joint analysis, these proteins (BDKRB1, CHRM4, EDN1, FOS, HRH3, IFNG, MMP2, MYC, NOS2, TLR4, VAMP2, and VEGFA) were selected for computer simulation of RIM principal component targeting. The sequence of these twelve proteins was obtained from the UniProt databases (Universal Protein Resource) (UniProt Consortium, 2018). The UniProtKB IDs were as follows: BDKRB1 (Q38Q38), CHRM4 (P17200), EDN1 (F1NWA9), FOS (P11939), HRH3 (F1NVX2), IFNG (P49708), MMP2 (Q90611), MYC (P01109), NOS2 (Q90703), TLR4 (C4PCF3), VAMP2 (A0A1D5PLR5) and VEGFA (P67964).

As the 3D structure of these five proteins (*Gallus gallus*) has not been elucidated yet, the method of comparative modeling was used for their 3D structure (Arnold, et al., 2006; Guex, et al., 2009) to construct the model using the alignment mode. We used PyMol (Delano, 2002) to erase the heteroatoms, water molecules, and inhibitor present in the structure and saved as a PDB file. The 3D structures of the ligand molecule were stored as a Mol2 or SDF file with the help of the TCMSP databases (Ru, et al., 2014) and PubChem (<https://pubchem.ncbi.nlm.nih.gov/>). The non-bonding interaction of ligand-protease was calculated using Autodock Vina software package (Trott and Olson, 2010) for docking analysis. After docking, the interaction of the five proteins and baicalin with the lowest affinity score for the receptors were selected for further analysis as mentioned in our previous study (Wu, et al., 2020).

#### Statistical analysis

Data are presented as mean results  $\pm$  standard deviation (SD). All the experiments were performed in triplicates (n = 3) unless otherwise mentioned. The significance was determined using one-way ANOVA followed by Dunnett's T3 test. The data were analyzed by using the GraphPad Prism (version 5.01). Values with  $p < 0.05$  were considered statistically significant. Heatmaps were made by Heatmap Illustrator software (1.03.7).

## Results

#### Component compounds of mixed herbs aqueous extraction

Utilizing a non-targeted metabolomics approach, we investigated the

aqueous extraction of compounds, revealing a diverse chemical profile. Our preceding study, employing UPLC-QTOF-MS/MS, detected a total of 260 compounds in the extract, encompassing both positive and negative ionization modes. This chemical inventory included a significant representation of flavonoids, with 85 compounds identified, organic acids with 64 compounds, phenylpropanoids with 17 compounds, and others. A comprehensive compilation of the compositional data for the mixed herbs is furnished in Supplementary Material 2.

Additionally, we conducted a screening to identify compounds with higher concentrations, as evidenced by the total ion current across both positive and negative ion modes, which is depicted in Fig. 1. The two-dimensional (2D) structural information for these ingredients was sourced from the PubChem database (<https://pubchem.ncbi.nlm.nih.gov/>), and the data were subsequently saved as SDF (Structure Data File) format for use in subsequent experimental analyses.

### Multi-omics joint analysis of co-infection

To delve into the metabolic shifts induced by co-infection, we deployed a UPLC-QTOF-MS/MS-based metabolomics approach to scrutinize alterations in serum metabolites. The non-targeted metabolomics data from the co-infection cohort revealed significant changes, with 245 metabolites (58 upregulated and 187 downregulated) identified in the positive mode and 882 metabolites (234 upregulated and 648 downregulated) in the negative mode (Wu, et al., 2020). Concurrently, we integrated the previously identified 57 key target genes and differential metabolites into MetaboAnalyst (version 4.0) for an advanced multi-omics joint analysis. The resulting gene-metabolite network is illustrated in Fig. 2A. Within this network, we prioritized metabolites and genes with the highest node association degree for further targeted verification across multiple dimensions.

### Effects of mixed herbs on the expression of genes and proteins in the lung

Based on the gene-metabolite network analysis, we identified 12 genes that were selected for further investigation into the mechanisms

underlying the positive effects of RIM on the target organ. These genes were utilized to generate a heatmap illustrating the relationships among the three experimental groups, as depicted in Fig. 2B. The heatmap reveals varying levels of chemokine and mucin expression surges in the co-infection group, with the exception of CHRM4, MMP2, and VEGFA, which did not exhibit this trend. Notably, in the Co-infection + RIM group, there was a significant reduction observed in the expression levels of approximately half of the genes studied.

In our quest for deeper insights, we pinpointed six pivotal proteins within the network for Western Blot (WB) experimentation: BDKRB1, EDN1, MMP2, TLR4, c-FOS, and VEGFA. Analysis of the expression levels of these proteins, as illustrated in Fig. 2C and D, revealed that the majority were significantly upregulated ( $0.01 < p < 0.05$ ) in the co-infection group when juxtaposed with the control groups, with the exception of c-FOS. Notably, EDN1, MMP2, and VEGFA exhibited extraordinarily significant expression levels ( $p < 0.01$ ). Upon RIM intervention, the expression of these target proteins was markedly downregulated relative to the co-infection group. It is noteworthy that RIM significantly modulated the expression of select genes and their corresponding proteins, particularly MMP2 and TLR4, with a high level of statistical significance ( $p < 0.01$ ).

### Expression of RIM on the key metabolites in the serum

We have previously established that Leukotriene C4 (LTC4) in serum serves as a reliable biomarker for diagnosing poultry respiratory diseases (Wu, et al., 2020). In conjunction with the findings from our transcriptome-metabonomic network analysis, we selected three additional metabolites—Dopamine,  $\gamma$ -Aminobutyric acid (GABA), and Leukotriene C4—for further investigation at the metabolic level. As depicted in Fig. 2E and F, there was a significant upregulation ( $p < 0.01$ ) in the expression of these three metabolites when comparing the Control group to the Co-infection group. Notably, following RIM treatment, there was a significant reduction ( $p < 0.05$ ) in the levels of Dopamine and GABA compared to the Co-infection group. However, the expression of LTC4 remained unchanged and did not reach significance even after

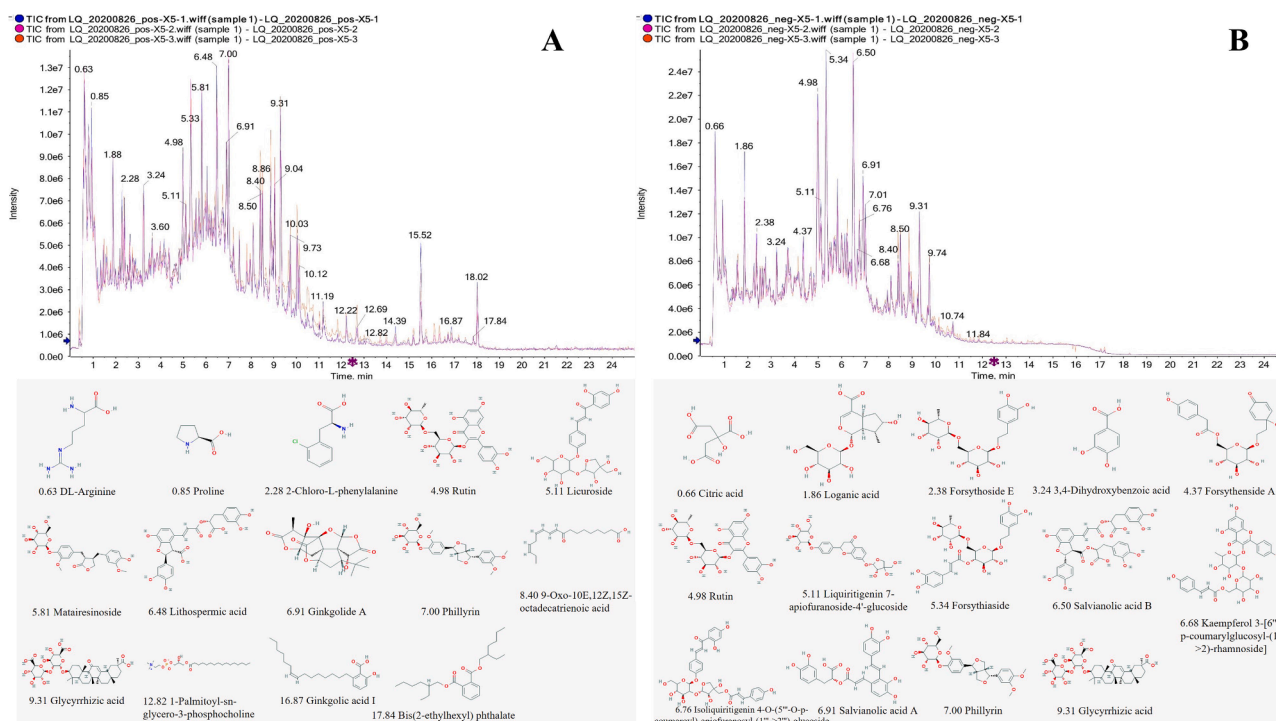
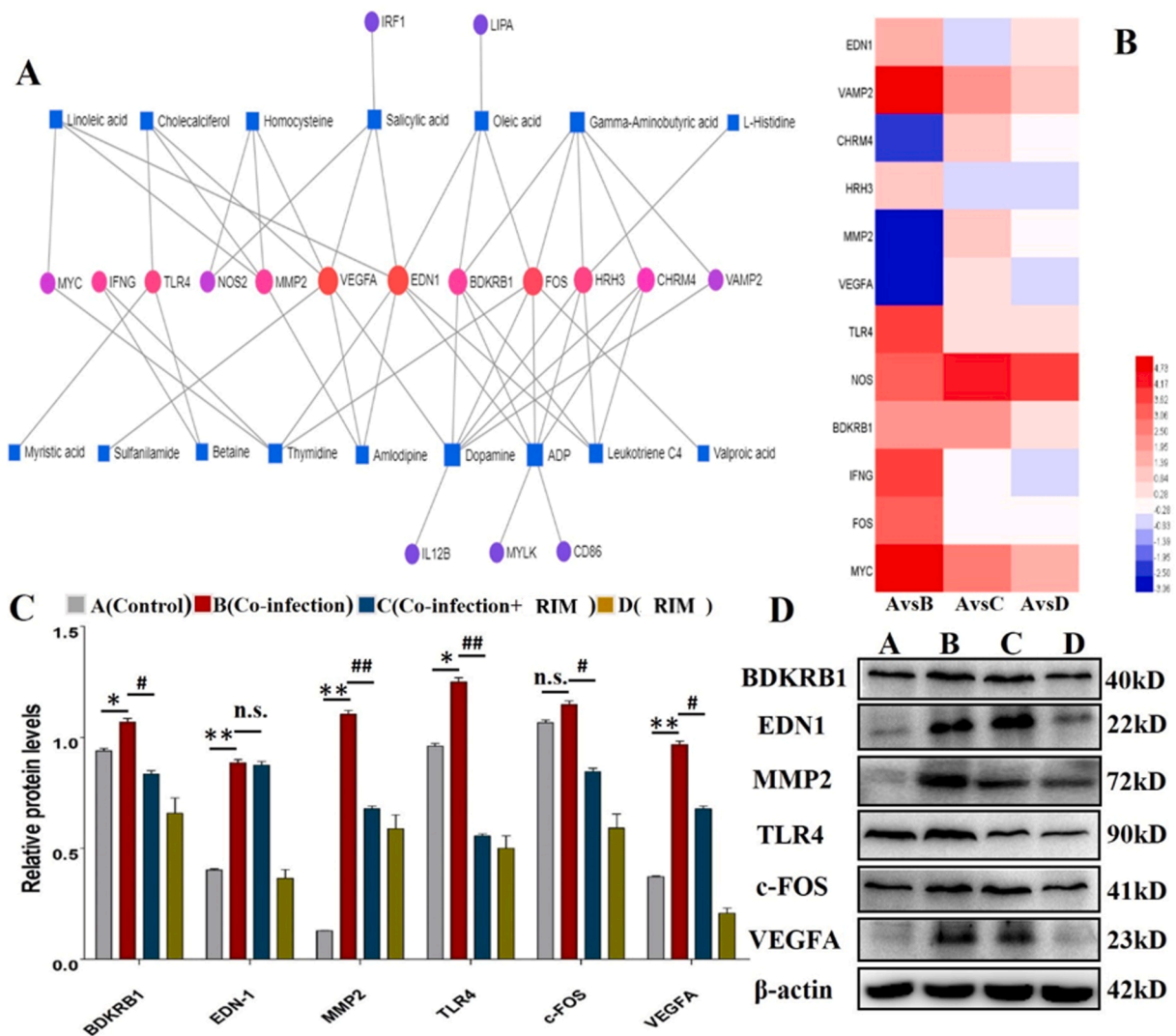


Fig. 1. Total ion chromatography in positive (A) and negative (B) ion modes. The 2D structure of main active ingredients as shown below in the chromatogram, and the decimal represent the peak times.



**Fig. 2.** (A) The gene-metabolite joint analysis network. The circles represent genes and the squares represent metabolites. Both the size and the shade of the color indicate the degree from big to small. (B) Heatmap showing the relative gene expression of target genes. A bright red color indicates a stronger up-regulation and a bright blue color indicates a stronger down-regulation in expression. (C) and (D) The protein levels of BDKRB1, EDN1, MMP2, TLR4, c-FOS and VEGFA were measured by western blot.  $\beta$ -actin was used as an internal control. (E) and (F) Three metabolites (Dopamine,  $\gamma$ -Aminobutyric acid and Leukotriene C4) of chromatogram in four groups by UPLC-MS. Bars represent the mean  $\pm$  SD. Bars with different superscript letters are significantly different ( $0.01 < p < 0.05$ ). The original figures (including western blot and UPLC/MS) were provided in Supplementary material 3.

RIM treatment. The original data, including Western blot and UPLC/MS results, are detailed in Supplementary Material 3.

#### Molecular docking of effective compounds and target proteins

Our non-targeted metabolomics analysis of RIM yielded a total of 21 potent compounds, encompassing both negative (NEG) and positive (POS) modes. We proceeded to conduct molecular docking studies on these 21 compounds with 12 key proteins. The compounds that demonstrated the highest absolute docking scores across all 12 key proteins were identified as potential candidate inhibitors. The original docking figures and detailed docking scores are available in Supplementary Material 4. Utilizing PyMol, we generated the optimal ligand-receptor complexes, and the interactions were further analyzed using the Protein-Ligand Interaction Profiler tool (Salentin, et al., 2015), as shown in Fig. 3. These results underscore the multifaceted nature of RIM, characterized by the interaction of multiple compounds with a single target and a single compound with multiple targets. Notably,

Salvianolic acid A ( $-10.1$  kcal/mol), Liquiritigenin ( $-9.3$  kcal/mol), and Isoliquiritigenin ( $-8.7$  kcal/mol) exhibited the lowest docking scores, indicating their potential to strongly bind to the active sites of the target proteins.

#### Discussion

We conducted multi-dimensional validations of targeted therapy across various biological levels, including gene, protein, and metabolite assessments, complemented by in vitro computer simulations. Subsequent to these analyses, we performed a joint examination of transcriptomics and metabolomics data, which facilitated the construction of a network map highlighting key genes and metabolites. Recent studies have emphasized that the integration of metabolomics and transcriptomics provides a sensitive and insightful approach to linking infection mechanisms with the biological responses they elicit (Chung, et al., 2021; Gardinassi, et al., 2018; Go, et al., 2018). In our study, we strategically selected the first 12 target genes exhibiting the highest

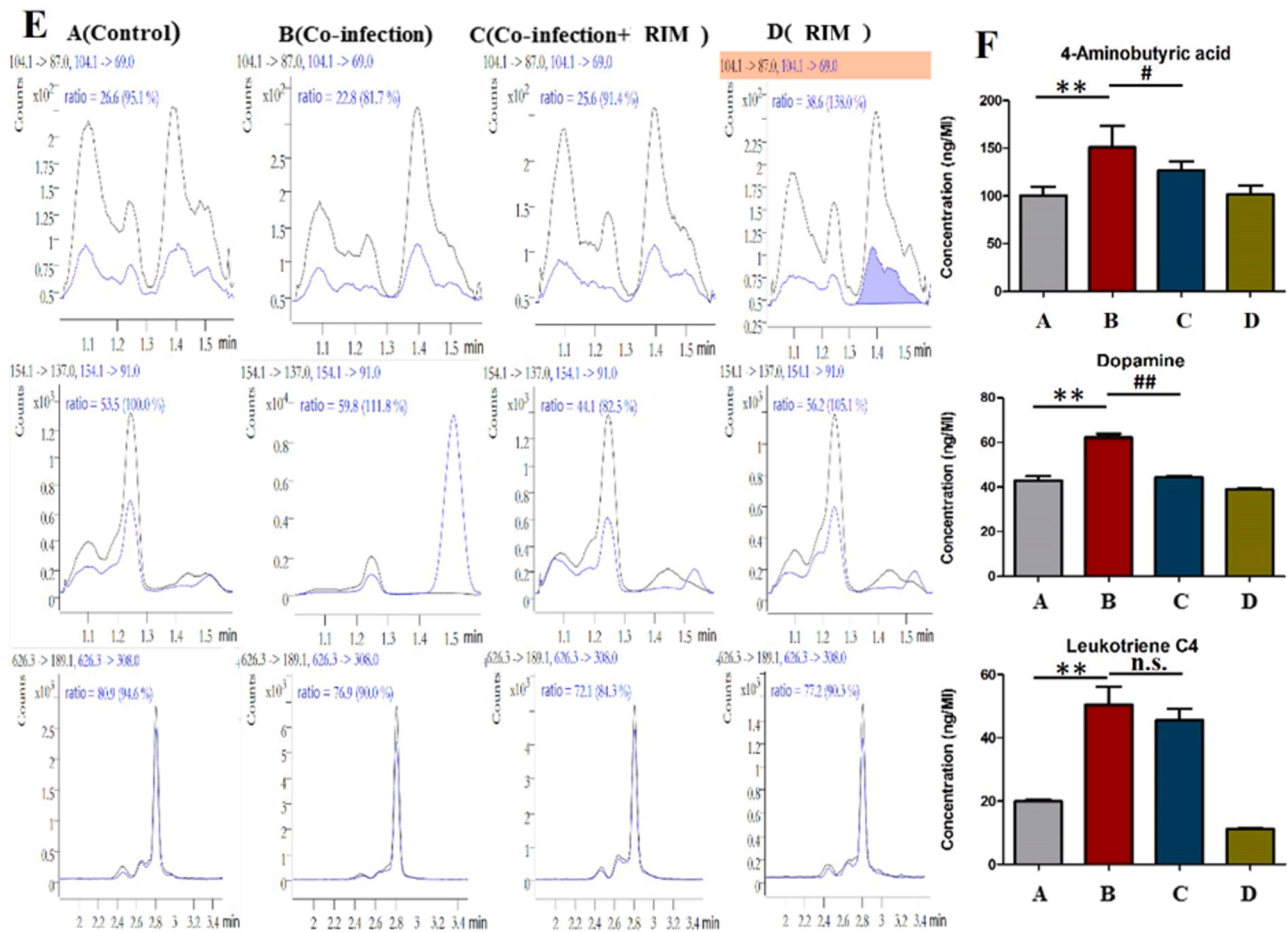


Fig. 2. (continued).

correlation degree for quantitative detection via reverse transcription polymerase chain reaction (RT-PCR). Our findings indicated a reduction in the expression levels of these genes following treatment. A substantial body of research has shown that these genes are essential components of a broad and dynamic network within the transcriptome, highlighting their regulatory functions (Sun, et al., 2020; Wu, et al., 2024). However, we observed contrasting results for the expression of CHRM4, MMP2, and VEGFA. To further validate these findings at the protein level, we conducted Western blot analysis. The results corroborated similar expression trends for the six proteins of interest: MMP2, TLR4, c-FOS, BDKRB1, VEGFA, and EDN1. The quantitative analysis of these targets suggested that the aqueous extract of RIM possesses a multi-target therapeutic potential. This was confirmed after an inverse screening process facilitated by network pharmacology.

Metabolites, as the most direct expression of biological reactions to external stimuli, it can effectively reflect changes in the upstream mechanisms of these biological processes (Cuadrado, et al., 2019; Yang, et al., 2020). Our prior metabolic findings have illuminated that the metabolism of Arachidonic Acid is heightened during co-infections, underscoring the potential of serum LTC4 to serve as a pivotal biomarker in the detection of avian respiratory ailments (Wu, et al., 2020). Drawing from an integrated analysis of transcriptomic and metabolomic data, the selection of Dopamine,  $\gamma$ -Aminobutyric acid, and Leukotriene C4 for further investigation was deemed essential. Studies have indicated that bacterial infections can trigger a surge of Dopamine in the brain, which in turn activates NF- $\kappa$ B and primes the NLRP3 inflammasome within primary human macrophages (Chertkova, et al., 2018; Nolan, et al., 2019). Additionally, the research has brought to light that  $\gamma$ -Aminobutyric acid, the brain's principal inhibitory

neurotransmitter, possesses activating roles within the immune system (Fuks, et al., 2012). These findings are similar to the results of co-infection. Moreover, the expression levels of these three metabolites were notably reduced following treatment with RIM.

Ultimately, to ascertain the multi-target efficacy of the active constituents derived from RIM aqueous extracts, an *in vitro* molecular docking analysis was employed. The binding affinity was gauged by the molecular docking scores, with lower scores indicating a stronger binding capacity. The binding affinity was gauged by the molecular docking scores, with lower scores indicating a stronger binding capacity (Trott and Olson, 2010). Notably, the targeted therapeutic potential of Salvianolic acid A, Liquiritigenin, and Isoliquiritigenin warrants further exploration. Additionally, numerous naturally derived compounds currently in clinical trials or demonstrating promise in pre-clinical studies deserve further scrutiny (Liu, et al., 2020; Mok, et al., 2020). In this study, we conducted a multi-dimensional targeted validation based on the integrated analysis network, with preliminary findings revealing the multi-target and multi-pathway efficacy of RIM. These findings propose a novel approach to validating the target combinations of natural products, potentially optimizing their structural-activity profiles and yielding drug-like natural product derivatives.

Nonetheless, it is imperative to recognize several inherent limitations within our experimental and polypharmacological methodologies. Initially, the incomplete knowledge of natural product components sourced from public databases restricts our predictive capabilities regarding TCM extraction for those lacking known information. Additionally, MetaboAnalyst (version 4.0) was utilized to concurrently analyze genes and metabolites of interest within metabolic pathways. However, the current version only supports data from humans, mice,

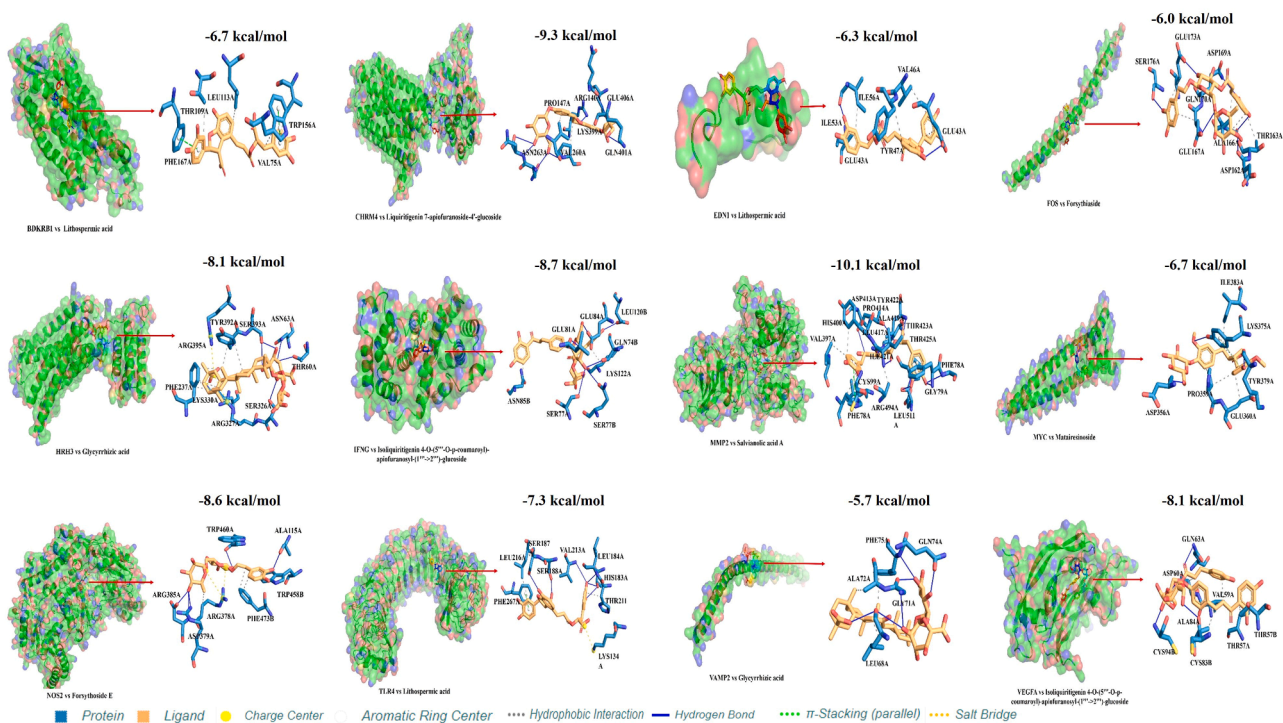


**Fig. 3.** 3D models of the optimum ligand and all 12 key proteins (pose predicted by AutoDock Vina; the interaction analysis was analyzed by Protein-Ligand Interaction Profiler). Blue solid line represents *Hydrogen Bond*, gray dotted line represents *Hydrophobic Interactions*, the dotted green line represents  *$\pi$ -Stacking*, the dotted yellow line represents *Salt Bridge*.

and rats (Chong, Wishart and Xia, 2019). Integrating the target network may facilitate the targeting of the burgeoning potential of co-infection genes by indirectly influencing neighboring proteins within the human interactome. Ultimately, the evolution of TCM must concentrate on an interdisciplinary approach, amalgamating research from burgeoning fields post-clarification of its material foundation. Regarding pharmacodynamics, elucidating the mechanisms of TCM extraction is essential, including an examination of the interplay between "Chinese herbal medicine, probiotics, and intestinal flora".

## Conclusion

Our research has demonstrated that RIM can exert pharmacological effects across multiple pathways and targets at various levels, including genes, proteins, metabolism, and molecular docking. Additionally, we highlight the potential of integrating transcriptomics and metabolomics analyses to identify therapeutic targets for co-infections. Finally, we provide a detailed verification of the complex pharmacological characteristics of RIM, offering a significant reference for future investigations into its pharmacological mechanisms.

## Ethics approval and consent to participate

Animal experiments were conducted in compliance with the regulations of the Laboratory Animal Ethics Committee of Northeastern Agricultural University (approved No.: NEAUEC20220324, approved date: Mar. 10, 2022).

## Confidentiality of data

The authors declare that no patient data appears in this article.

## Authors contributions

XJ and ZW designed the study. YY, MS and RL performed and

collected data from experiment and analyzed data. XJ and JH wrote the manuscript. All authors read and approved the final manuscript.

## Disclosures

The authors declare no conflicts of interest and no competing financial interests.

## Acknowledgments

This research was supported by the Natural Science Foundation of Heilongjiang Province (LH2022C038), Special Funding for Postdoctoral of Heilongjiang Province (LBH-TZ2119) and the National Natural Science Foundation of China (32473096).

## Supplementary materials

Supplementary material associated with this article can be found, in the online version, at [doi:10.1016/j.psj.2024.104576](https://doi.org/10.1016/j.psj.2024.104576).

## References

- Amirteymoori, E., A. Khezri, O. Dayani, M. Mohammadabadi, S. Khorasani, A. Mousaie, and M. Kazemi-Bonchenari. Effects of linseed processing method (ground versus extruded) and dietary crude protein content on performance, digestibility, ruminal fermentation pattern, and rumen protozoa population in growing lambs. 2021.
- Arnold, K., Bordoli, L., Kopp, J., Schwede, T., 2006. The SWISS-MODEL workspace: a web-based environment for protein structure homology modelling. *Bioinformatics*. 22, 195–201. <https://doi.org/10.1093/bioinformatics/bti770>.
- Awad, N.F.S., Abd El-Hamid, M.I., Hashem, Y.M., Erfan, A.M., Abdelrahman, B.A., Mahmoud, H.I., 2019. Impact of single and mixed infections with *Escherichia coli* and *Mycoplasma gallisepticum* on Newcastle disease virus vaccine performance in broiler chickens: an in vivo perspective. *J. Appl. Microbiol.* 127, 396–405. <https://doi.org/10.1111/jam.14303>.
- Bai, D.P., Lin, X.Y., Huang, Y.F., Zhang, X.F., 2018. Theranostics aspects of various nanoparticles in veterinary medicine. *Int. J. Mol. Sci.* 19. <https://doi.org/10.3390/ijms19113299>.
- Bao, J., Wang, Y., Wang, S., Niu, D., Wang, Z., Li, R., Zheng, Y., Ishfaq, M., Wu, Z., Li, J., 2022. Polypharmacology-based approach for screening TCM against coinfection of

- Mycoplasma gallisepticum and Escherichia coli. *Front. Vet. Sci.* 9, 972245. <https://doi.org/10.3389/fvets.2022.972245>.
- Cao, Y., Shi, J., Song, L., Xu, J., Lu, H., Sun, J., Hou, J., Chen, J., Wu, W., Gong, L., 2022. Multi-Omics integration analysis identifies lipid disorder of a non-alcoholic fatty liver disease (NAFLD) mouse model improved by Zexie-Baizhu decoction. *Front. Pharmacol.* 13, 858795. <https://doi.org/10.3389/fphar.2022.858795>.
- Chertkova, E.A., Grizanova, E.V., Dubovskiy, I.M., 2018. Bacterial and fungal infections induce bursts of dopamine in the haemolymph of the Colorado potato beetle *Leptinotarsa decemlineata* and greater wax moth *Galleria mellonella*. *J. Invertebr. Pathol.* 153, 203–206. <https://doi.org/10.1016/j.jip.2018.02.020>.
- Chong, J., Soufan, O., Li, C., Caraus, I., Li, S., Bourque, G., Wishart, D.S., Xia, J., 2018. MetaboAnalyst 4.0: towards more transparent and integrative metabolomics analysis. *Nucleic. Acids. Res.* 46, W486–w494. <https://doi.org/10.1093/nar/gky310>.
- Chong, J., D. S. Wishart, and J. Xia. 2019. Using MetaboAnalyst 4.0 for comprehensive and integrative metabolomics data analysis. 2019/11/23 ed.
- Chung, P.Y., Khoo, R.E.Y., Liew, H.S., Low, M.L., 2021. Antimicrobial and antibiofilm activities of Cu(II) Schiff base complexes against methicillin-susceptible and resistant *Staphylococcus aureus*. *Ann. Clin. Microbiol. Antimicrob.* 20, 67. <https://doi.org/10.1186/s12941-021-00473-4>.
- Cuadrado, A., Rojo, A.I., Wells, G., Hayes, J.D., Cousin, S.P., Rumsey, W.L., Attucks, O.C., Franklin, S., Levonen, A.L., Kensler, T.W., Dinkova-Kostova, A.T., 2019. Therapeutic targeting of the NRF2 and KEAP1 partnership in chronic diseases. *Nat. Rev. Drug Discov.* 18, 295–317. <https://doi.org/10.1038/s41573-018-0008-x>.
- Delano, W. L. 2002. The PyMol Molecular Graphics System. 30:442–454.
- Fuks, J.M., Arrighi, R.B., Weidner, J.M., Kumar Mendu, S., Jin, Z., Wallin, R.P., Rethi, B., Birmir, B., Barragan, A., 2012. GABAergic signaling is linked to a hypermigratory phenotype in dendritic cells infected by *Toxoplasma gondii*. *PLoS. Pathog.* 8, e1003051. <https://doi.org/10.1371/journal.ppat.1003051>.
- Gardinassi, L.G., Arévalo-Herrera, M., Herrera, S., Cordy, R.J., Tran, V., Smith, M.R., Johnson, M.S., Chacko, B., Liu, K.H., Darley-Usmar, V.M., Go, Y.M., Jones, D.P., Galinski, M.R., Li, S., 2018. Integrative metabolomics and transcriptomics signatures of clinical tolerance to Plasmodium vivax reveal activation of innate cell immunity and T cell signaling. *Redox. Biol.* 17, 158–170. <https://doi.org/10.1016/j.redox.2018.04.011>.
- Gharibi, D., Ghadimipour, R., Mayahi, M., 2018. Detection of *Mycoplasma gallisepticum* and *Mycoplasma synoviae* among commercial Poultry in Khouzestan Province, Iran. *Arch. Razi. Inst.* 73, 139–146. <https://doi.org/10.22092/ari.2018.116164>.
- Go, Y.M., Fernandes, J., Hu, X., Uppal, K., Jones, D.P., 2018. Mitochondrial network responses in oxidative physiology and disease. *Free Radic. Biol. Med.* 116, 31–40. <https://doi.org/10.1016/j.freeradbiomed.2018.01.005>.
- Guex, N., Peitsch, M.C., Schwede, T., 2009. Automated comparative protein structure modeling with SWISS-MODEL and Swiss-PdbViewer: a historical perspective. *Electrophoresis* 30 (Suppl 1), S162–S173. <https://doi.org/10.1002/elps.200900140>.
- Gul, S. T., and A. F. J. P. V. J. Alsayeqh. 2022. Probiotics as an alternative approach to antibiotics for safe poultry meat production. 42:285–291.
- Hu, W., W. Zhang, S. Shah, M. Ishfaq, J. L. J. Developmental, and C. Immunology. 2020. *Mycoplasma gallisepticum* infection triggered histopathological changes, oxidative stress and apoptosis in chicken thymus and spleen. 114:103832.
- Ishfaq, M., Chen, C., Bao, J., Zhang, W., Wu, Z., Wang, J., Liu, Y., Tian, E., Hamid, S., Li, R., Ding, L., Li, J., 2019. Baicalin ameliorates oxidative stress and apoptosis by restoring mitochondrial dynamics in the spleen of chickens via the opposite modulation of NF-kappaB and Nrf2/HO-1 signaling pathway during *Mycoplasma gallisepticum* infection. *Poult. Sci.* 98, 6296–6310. <https://doi.org/10.3382/ps/pez406>.
- Ishfaq, M., Zhang, W., Liu, Y., Wang, J., Wu, Z., Ali Shah, S.W., Li, R., Miao, Y., Chen, C., Li, J., 2020. Baicalin attenuated *Mycoplasma gallisepticum*-induced immune impairment in the chicken Bursa of Fabricius through modulation of autophagy and inhibited inflammation and apoptosis. *J. Sci. Food Agric.* <https://doi.org/10.1002/jsfa.10695>.
- Ji, H.Y., Liu, K.H., Kong, T.Y., Jeong, H.U., Choi, S.Z., Son, M., Cho, Y.Y., Lee, H.S., 2013. Evaluation of DA-9801, a new herbal drug for diabetic neuropathy, on metabolism-mediated interaction. *Arch. Pharm. Res.* 36, 1–5. <https://doi.org/10.1007/s12272-013-0014-9>.
- Jin, W., Zhou, T., Li, G., 2019. Recent advances of modern sample preparation techniques for traditional Chinese medicines. *J. Chromatogr. A* 1606, 460377. <https://doi.org/10.1016/j.chroma.2019.460377>.
- Kenton, and K. r. a. J. I. P. Production. 2012. Management of respiratory diseases in poultry. 20:11–13.
- Kou, J., Zhu, D., Yan, Y., 2005. Neuroprotective effects of the aqueous extract of the Chinese medicine Danggui-Shaoyao-san on aged mice. *J. Ethnopharmacol.* 97, 313–318. <https://doi.org/10.1016/j.jep.2004.11.020>.
- Langeder, J., Grienke, U., Chen, Y., Kirchmair, J., Schmidtke, M., Rollinger, J.M., 2020. Natural products against acute respiratory infections: strategies and lessons learned. *J. Ethnopharmacol.* 248, 112298. <https://doi.org/10.1016/j.jep.2019.112298>.
- Li, X., X. Zhu, and Y. J. P. V. J. Xue. 2023. Drug resistance and genetic relatedness of *Escherichia coli* from Mink in Northeast China. 43:824–827.
- Liu, N., Wu, C., Jia, R., Cai, G., Wang, Y., Zhou, L., Ji, Q., Sui, H., Zeng, P., Xiao, H., Liu, H., Huo, J., Feng, Y., Deng, W., Li, Q., 2020. Traditional Chinese medicine combined with chemotherapy and Cetuximab or Bevacizumab for metastatic colorectal cancer: a randomized, double-blind, placebo-controlled clinical trial. *Front. Pharmacol.* 11, 478. <https://doi.org/10.3389/fphar.2020.00478>.
- Moazeni, S. M., M. Mohammadabadi, M. Sadeghi, H. M. Shahrabak, A. E. Koshkoieh, and F. J. O. J. o. A. e. Bordbar. 2016. Association between UCP gene polymorphisms and growth, breeding value of growth and reproductive traits in Mazandaran indigenous chicken. 6:1–8.
- Mohammadabadi, M. R., M. Nikbakhti, H. R. Mirzaee, M. A. Shandi, and I. G. J. G. Moiseyeva. 2010. Genetic variability in three native Iranian chicken populations of the Khorasan province based on microsatellite markers. 46:572–576.
- Mohammadifar, A., S. A. Faghil Imani, M. R. Mohammadabadi, and M. J. C. J. o. A. B. Soflaei. 2014. The effect of TGFβ3 gene on phenotypic and breeding values of body weight traits in Fars native fowls. 5:125–136.
- Mohammadifar, A., and M. J. M. A. B. Mohammadabadi. 2018. Melanocortin-3 receptor (MC3R) gene association with growth and egg production traits in fars indigenous chicken. 47.
- Mok, S.W., Wong, V.K., Lo, H.H., de Seabra Rodrigues Dias, I.R., Leung, E.L., Law, B.Y., Liu, L., 2020. Natural products-based polypharmacological modulation of the peripheral immune system for the treatment of neuropsychiatric disorders. *Pharmacol. Ther.* 208, 107480. <https://doi.org/10.1016/j.pharmthera.2020.107480>.
- Mol, N., Peng, L., Esnault, E., Quere, P., Haagsman, H.P., Veldhuizen, E.J.A., 2019. Avian pathogenic *Escherichia coli* infection of a chicken lung epithelial cell line. *Vet. Immunol. Immunopathol.* 210, 55–59. <https://doi.org/10.1016/j.vetimm.2019.03.007>.
- Nolan, R. A., K. L. Reeb, Y. Rong, S. M. Matt, P. J. J. B. B. Gaskill, and I.-. Health. 2019. Dopamine activates NF-κB and primes the NLRP3 inflammasome in primary human macrophages. 2:100030.
- Pan, L., Li, Z., Wang, Y., Zhang, B., Liu, G., Liu, J., 2020. Network pharmacology and metabolomics study on the intervention of traditional Chinese medicine Huanglian Decoction in rats with type 2 diabetes mellitus. *J. Ethnopharmacol.* 258, 112842. <https://doi.org/10.1016/j.jep.2020.112842>.
- Plichta, D.R., Graham, D.B., Subramanian, S., Xavier, R.J., 2019. Therapeutic opportunities in inflammatory bowel disease: mechanistic dissection of host-microbiome relationships. *Cell* 178, 1041–1056. <https://doi.org/10.1016/j.cell.2019.07.045>.
- Rehman, A.U., Shah, A.H., Rahman, S.U., Khan, S., UllahUllah, I., Farid, Q., Khan, A., Hashim, M., 2022. Molecular confirmation and immunological cross reactivity among *Mycoplasma gallisepticum* isolates recovered from broiler chicken in Khyber Pakhtunkhwa, Pakistan. % *J Pakistan Veterinary Journal* 42, 487–492.
- Ru, J., Li, P., Wang, J., Zhou, W., Li, B., Huang, C., Li, P., Guo, Z., Tao, W., Yang, Y., Xu, X., Li, Y., Wang, Y., Yang, L., 2014. TCMSP: a database of systems pharmacology for drug discovery from herbal medicines. *J. Cheminform.* 6, 13. <https://doi.org/10.1186/1758-2946-6-13>.
- Salentin, S., Schreiber, S., Haupt, V.J., Adasme, M.F., Schroeder, M., 2015. PLIP: fully automated protein-ligand interaction profiler. *Nucleic. Acids. Res.* 43, W443–W447. <https://doi.org/10.1093/nar/gkv315>.
- Sanchez-Vidana, D.I., Rajwani, R., Wong, M.S., 2017. The use of omic technologies applied to traditional Chinese medicine research. *Evid. Based. Complement. Alternat. Med.* 2017, 6359730. <https://doi.org/10.1155/2017/6359730>.
- Sid, H., Benachour, K., Rautenschlein, S., 2015. Co-infection with multiple Respiratory pathogens contributes to increased mortality rates in Algerian poultry flocks. *Avian Dis.* 59, 440–446. <https://doi.org/10.1637/11063-031615-Case.1>.
- Sun, D.P., Lee, Y.W., Chen, J.T., Lin, Y.W., Chen, R.M., 2020. The bradykinin-BDKRB1 axis regulates aquaporin 4 gene expression and consequential migration and invasion of malignant glioblastoma cells via a Ca(2+)-MEK1-ERK1/2-NF-κB mechanism. *Cancers. (Basel)* 12. <https://doi.org/10.3390/cancers12030667>.
- Sun, Q., Wu, S., Liu, K., Li, Y., Mehmood, K., Nazari, M., Hu, L., Pan, J., Tang, Z., Liao, J., Zhang, H., 2023. miR-181b-1-3p affects the proliferation and differentiation of chondrocytes in TD broilers through the WIF1/Wnt/β-catenin pathway. *Pestic. Biochem. Physiol.* 197, 105649. <https://doi.org/10.1016/j.pestbp.2023.105649>.
- Telli, A.E., Bicer, Y., Telli, G.O., Ertas, N., 2022. Pathogenic *Escherichia coli* and *Salmonella* spp. In Chicken carcass rinses: isolation and genotyping by ERIC-PCR. % *J Pakistan Veterinary Journal* 42, 493–498.
- Trott, O., Olson, A.J., 2010. AutoDock Vina: improving the speed and accuracy of docking with a new scoring function, efficient optimization, and multithreading. *J. Comput. Chem.* 31, 455–461. <https://doi.org/10.1002/jcc.21334>.
- Umar, S., Delverdier, M., Delpont, M., Belkasm, S.F.Z., Teillaud, A., Bleuart, C., Pardo, I., El Houadfi, M., Guerin, J.L., Ducatez, M.F., 2018. Co-infection of turkeys with *Escherichia coli* (O78) and H6N1 avian influenza virus. *Avian Pathology: Journal of the W.V.P.A.* 47, 314–324. <https://doi.org/10.1080/03079457.2018.1449942>.
- Umar, S., Teillaud, A., Aslam, H.B., Guerin, J.L., Ducatez, M.F., 2019. Molecular epidemiology of respiratory viruses in commercial chicken flocks in Pakistan from 2014 through to 2016. *BMC. Vet. Res.* 15, 351. <https://doi.org/10.1186/s12917-019-2103-6>.
- UniProt Consortium, T., 2018. UniProt: the universal protein knowledgebase. *Nucleic. Acids. Res.* 46, 2699. <https://doi.org/10.1093/nar/gky092>.
- Wang, J., M. Ishfaq, and J. Li. Baicalin ameliorates *Mycoplasma gallisepticum*-induced inflammatory injury in the chicken lung through regulating the intestinal microbiota and phenylalanine metabolism. 2021.
- Wang, Y., Chen, S., Yu, O., 2011. Metabolic engineering of flavonoids in plants and microorganisms. *Appl. Microbiol. Biotechnol.* 91, 949–956. <https://doi.org/10.1007/s00253-011-3449-2>.
- Wang, Y.S., Shen, C.Y., Jiang, J.G., 2019. Antidepressant active ingredients from herbs and nutraceuticals used in TCM: pharmacological mechanisms and prospects for drug discovery. *Pharmacol. Res.* 150, 104520. <https://doi.org/10.1016/j.phrs.2019.104520>.
- Wu, S., Liu, K., Huang, X., Sun, Q., Wu, X., Mehmood, K., Li, Y., Zhang, H., 2024. Molecular mechanism of miR-203a targeting Runx2 to regulate thiram induced-chondrocyte development. *Pestic. Biochem. Physiol.* 200, 105817. <https://doi.org/10.1016/j.pestbp.2024.105817>.
- Wu, Z., C. Chen, Q. Zhang, J. Bao, Q. Fan, R. Li, M. Ishfaq, and J. Li. 2020. Arachidonic acid metabolism is elevated in *Mycoplasma gallisepticum* and *Escherichia coli* co-



- infection and induces LTC4 in serum as the biomarker for detecting poultry respiratory disease. 2020/05/23 ed.
- Wu, Z., L. Ding, J. Bao, Y. Liu, Q. Zhang, J. Wang, R. Li, M. Ishfaq, and J. Li. 2019. Co-infection of *Mycoplasma gallisepticum* and *Escherichia coli* triggers inflammatory injury involving the IL-17 signaling pathway. 10. doi [10.3389/fmicb.2019.02615](https://doi.org/10.3389/fmicb.2019.02615).
- Yang, F., DeLuca, J.A.A., Menon, R., Garcia-Vilarato, E., Callaway, E., Landrock, K.K., Lee, K., Safe, S.H., Chapkin, R.S., Allred, C.D., Jayaraman, A., 2020. Effect of diet and intestinal AhR expression on fecal microbiome and metabolomic profiles. *Microb. Cell Fact.* 19, 219. <https://doi.org/10.1186/s12934-020-01463-5>.
- Yin, J.B., Zhou, K.C., Wu, H.H., Hu, W., Ding, T., Zhang, T., Wang, L.Y., Kou, J.P., Kaye, A.D., Wang, W., 2016. Analgesic effects of Danggui-Shaoyao-San on various "phenotypes" of nociception and inflammation in a Formalin pain model. *Mol. Neurobiol.* 53, 6835–6848. <https://doi.org/10.1007/s12035-015-9606-3>.
- Zhang, W., Y. Liu, Q. Zhang, S. Shah, and J. J. F. i. V. S. Li. 2020. *Mycoplasma gallisepticum* infection impaired the structural integrity and immune function of bursa of Fabricius in chicken: implication of oxidative stress and apoptosis. 7:225.
- Zheng, H., Pan, L., Xu, P., Zhu, J., Wang, R., Zhu, W., Hu, Y., Gao, H., 2017. An NMR-based metabolomic approach to unravel the preventive effect of water-soluble extract from *Dendrobium officinale* Kimura & Migo on streptozotocin-induced diabetes in mice. *Molecules.* 22. <https://doi.org/10.3390/molecules22091543>.